Volume 22, No 3 | International Journal of Radiation Research, July 2024

Estimating the relative biological effectiveness of light ions using TOPAS monte carlo simulation

M. Arif Efendi[1,2], D. Sakata[3], Y.C. Keat[1*]

[1]*Department of Biomedical Imaging, Advanced Medical and Dental Institute, Universiti Sains Malaysia, Penang, Malaysia*

[2]*Department of Nuclear Engineering and Engineering Physics, Faculty of Engineering, Universitas Gadjah Mada, Yogyakarta, Indonesia*

[3]*Division of Health Sciences, Graduate School of Medicine, Osaka University, Osaka, Japan*

► ***Original article***

Corresponding author:
Ying Chee Keat, Ph.D.,
E-mail: *ckying7@usm.my*

Received: May 2023
Final revised: December 2023
Accepted: March 2024

Int. J. Radiat. Res., July 2024; 22(3): 703-709

DOI: 10.61186/ijrr.22.3.703

Keywords: *Helium ion, Modified MKM, NSRL, Proton, TOPAS.*

ABSTRACT

Background: This paper presents a Monte Carlo (MC) simulation study estimating Relative Biological Effectiveness at a 10% survival fraction (RBE10) of light ion beams by means of microdosimetric approach. Microdosimetric parameters for estimating Relative Biological Effectiveness (RBE) were determined through the utilisation of the Tool for Particle Simulation (TOPAS) MC simulations. These simulations incorporated a 3D silicon on insulator (SOI) Bridge microdosimeter model. ***Materials and Methods:*** The incident 176.8 MeV proton and 176.4 MeV/u helium ion beams were simulated at different depths within a water phantom. The microdosimetric aspects, such as y_F^- and y_D^- at different depths along the fields were predicted from simulations. The RBE10 were derived using simulated microdosimetric spectra as inputs to the modified Microdosimetric Kinetic Model (MKM). ***Results:*** Simulated y_D^- distributions for proton and helium ion beams in water were about 4 keV/µm and 4 to 8 keV/µm at the plateau region, respectively and around 7 to 14 keV/µm and 35 to 56 keV/µm at the Bragg peak (BP) region, respectively. In the tail region y_D^- values were increasing from 5 keV/µm to 10 keV/µm and 7 keV/µm to 14 keV/µm at depths of 224 mm to 250 mm, respectively. ***Conclusion:*** The RBE10 for protons exhibit a range of 0.99 to 1.22, which differs from the standard practice of using a fixed RBE of 1.1 in the Treatment Planning System (TPS) for proton therapy. The simulation results in this study may be used as an outlook for radiobiological experiments in the NASA Space Radiation Laboratory (NSRL).

INTRODUCTION

The expanding number of charged particle therapy facilities and good clinical results have increased interest in charged particle radiation research initiatives worldwide [1–3] . The NSRL at Brookhaven National Laboratory [4] is the only United States research facility delivering multiple high-energy charged particle beams. It is increasingly being employed for fundamental radiobiological research involving various types of ions [5,6].

In charged particle beam treatments, it is essential to accurately estimate the biological effects on tumour and organs at risk (OAR). Microdosimetry along with MKM can be utilised to estimate the RBE [7]. In the clinical practice of proton therapy, RBE is assumed to be a constant 1.1 as a reference to photon radiotherapy [8]. However, proton beams present an increase in Linear Energy Transfer (LET) values which correspond to RBE and may vary along the beam path, especially at the distal edge of the BP [9].

Different types of microdosimeters have been developed to measure radiation dose at the microscopic level by measuring the energy deposition in Sensitive Volume (SV) e.g., Tissue Equivalent Proportional Counter (TEPC) [10], mini-TEPC [11], microdiamond [12], monolithic ΔE–E telescope [13], microcalorimeter [14], and silicon microdosimeter [15].

Numerous MC software have been created or expanded to incorporate the capability to simulate microdosimetric occurrences [16] , such as FLUKA [17], Geant4 [18–20], Geant4-DNA [21] , and MCNP6 [22]. Monte Carlo model for Heavy Ion Therapy (MCHIT) is built on top of the Geant4 version 8.2 developed at Goethe University Frankfurt, Germany [23]. MCHIT shows the ability to simulate microdosimetry spectra of carbon ion beams in water and PMMA phantom by using TEPC [24]. Zhu *et al.* [25] developed a microdosimetric extension in TOPAS for TEPC, mini TEPC, and SOI microdosimeter subsequently validated against experimental data.

The extensive use of MC simulation to model microdosimeter has been demonstrated in several publications. Bolst *et al.* [26] validate the Geant4 toolkit of silicon microdosimeter in therapeutic ion

[DOI: 10.61186/ijrr.22.3.703]

beams of carbon, nitrogen, and oxygen against experimental measurements. Geant4 exhibited a satisfactory level of concordance with experimental measurements, especially when considering regions preceding the distal boundary of the BP. However, there was a reduced level of consensus observed further downstream from the BP in both simulation and experiment, especially when considering carbon and oxygen ion beams. This disparity can be attributed to a greater presence of lighter fragments as opposed to heavier fragments. Overall, the findings demonstrate that Geant4 is a viable choice for simulating silicon microdosimetry in heavy ion therapy. Taddei *et al.* [27] compared the Geant4 MC simulation of energy deposition in spherical TEPC with experimental measurements. The data produced by the Geant4 simulation corresponded closely to the data obtained through measurement using a TEPC for particles entering the detector's centre and those near the gas-wall boundary. The frequency mean lineal energy (y_F^-) and dose mean lineal energy (y_D^-) values were within an 8% range of the measured data.

There are numerous MC simulation and RBE modelling studies for proton and helium ions [25,28–32]. Eulitz *et al.* [28] developed a MC model for simulating dose and Linear Energy Transfer (LET) distributions. They demonstrated the model's ability to accurately predict the average dose within the clinical target volume and water phantom dose measurements, achieving results within a 2% margin of accuracy. This research contributes to the development of a framework for modeling radiation responses, particularly in assessing the variable RBE in proton therapy. Bronk *et al.* [29] calculated the dose, dose-averaged linear energy transfer (LET_d), and y_D^- using a Geant4-based MC system that had been experimentally validated. The experiment involved exposing cells to protons, carbon ions, and helium ions at the Heidelberg Ion Beam Therapy Center (HIT), Germany. Their findings revealed that the clonogenic survival curves for all tested ions were influenced by y_D^-. Carbon and helium ions exhibited peak RBE values within specific y_D^- ranges before experiencing a decrease in biological efficacy, indicative of an overkill effect. In contrast, protons did not show an overkill effect, but their RBE increased as they moved distally from the BP. Importantly, the observed RBE profiles were closely linked to physical characteristics, such as y_D^-, and were ion-specific.

This study uses MC simulations to predict the microdosimetric quantities of proton and helium ion beams. RBE_{10} as a function of depth in a water phantom is analysed to determine beam quality for therapeutic irradiation. The results of this work could be used as an outlook for a future radiobiological experiment in NSRL. Furthermore, the results obtained from this study provide a new understanding of proton and helium ion RBE values, benchmarking of RBE models to accurately predict biological effect and cell survival for proton and helium ion beams, contributing to the limited dataset available for helium ions. The results could also support the commissioning of RBE used in TPS and quality assurance in the future.

MATERIALS AND METHODS

TOPAS simulation

The MC study has been performed using TOPAS version 3.7, TOPAS MC Inc., USA layered on top of Geant4 version 10.6.p3, European Organization for Nuclear Research (CERN), Switzerland [33,34]. The physics list implemented were g4em-standard_opt4, g4h-phy_QGSP_BIC_HP, g4em-extra, g4h-elastic_HP, g4stopping, g4ion-binarycascade, g4decay, and g4radioactivedecay.

This work included TOPAS microdosimetric extension [25], which contains a 3D SOI Bridge Microdosimeter developed at Centre for Medical Radiation Physics (CMRP), University of Wollongong (UOW), Australia to score energy deposition within micron SV. The proton and helium ion beams began with an initial energy of 176.8 MeV and 176.4 MeV/u, respectively. Their energy deviations were 0.3% and 0.1%, respectively.

A 10^7 histories were simulated to obtain the depth dose distributions in a water phantom. Pristine BP of proton and helium ion beams were compared to the experimental data taken in NSRL [6]. To simulate energy deposition in the detector for microdosimetry, we ran 10^7 histories before the BP and 10^8 histories at its distal edge and tail.

Modified MKM for RBE estimation

Microdosimetric quantities are determined by lineal energy (y) by converted energy deposition within a micron volume along the path of a particle. This is expressed mathematically as equation 1.

$$y = \frac{\varepsilon}{< l >} \quad (1)$$

where ε represents the amount of energy released during an individual occurrence within a SV, where this volume has a mean chord length denoted as $<l>$. In this work, a mean path length $<l_{path}>$ was used instead of $<l>$ as obtained by Geant4 MC simulation. Bolst *et al.* [35] proposed using the SV thickness to approximate the calculated $<l_{path}>$ values of 10 µm for a 3D SOI Bridge microdosimeter. Silicon to tissue correction factor of 0.58 obtained by Geant4 MC simulation was used to relate the mean chord length in silicon to tissue. The lineal energy (y) after implementing $<l_{path}>$ and correction factor (κ) is shown in equation 2.

$$y = \frac{\kappa\varepsilon}{< l_{path} >} \quad (2)$$

[DOI: 10.61186/ijrr.22.3.703]

The lineal energy (y) obtained from equation 2 was used to calculate dose lineal energy distribution $d(y)$ as given by the equation 3.

$$d(y) = \frac{y.f(y)}{\overline{yF}} \quad (3)$$

Where y_F^- is the frequency mean lineal energy defined by equation 4.

$$\overline{yF} = \int_0^\infty y.f(y)dy \quad (4)$$

The dose mean lineal energy (y_D^-) is the parameter to determine α parameter defined by equation 5.

$$\overline{yD} = \int_0^\infty y.d(y)dy \quad (5)$$

The modified MKM relates the dose mean lineal energy (y_D^-) to the Linear Quadratic Model (LQM) parameter α for a particular radiation field. Using the LQM, the RBE_{10} can be expressed as equation 6.

$$RBE_{10} = \frac{2\beta_{ref} D_{10,ref}}{\sqrt{\alpha_p^2 - 4\beta_{ref}\ln(0.1)} - \alpha_p} \quad (6)$$

Where α and β are tissue radio-sensitivity coefficients for radiation of interest and $D_{10,ref}$ is the 10% survival dose for Human Salivary Gland (HSG) tumour cells for which 200 kVp X-ray reference radiation is used.

RESULTS

Mono-energetic 176.8 MeV proton beams

Figure 1 compares the TOPAS simulation and NSRL experimental data of Bragg curves for mono-energetic 176.8 MeV proton beams in a water phantom. TOPAS MC simulation of Bragg curves has a good agreement with NSRL experimental data. The experiment started at a depth of 31.65 mm because of the limitation of the ionisation chamber's position in the phantom. The BP position of the TOPAS simulation occurs at a depth of 204.76 mm, while the experiment occurred at a depth of 204.95 mm. The difference between the simulation and experiment was 0.19 mm due to positioning uncertainty in the experiment setup.

The microdosimetric spectra of mono-energetic 176.8 MeV proton beams plotted as a function of lineal energy are present in figure 2. The spectra obtained were converted from silicon to water with a 3D Bridge SOI microdosimeter. It can be observed that the peak of the spectra shifts to a higher lineal energy range when the beam penetrated the water phantom, indicating increased LET of incident ions and contribution from secondary fragments.

Figure 3 (a) and (b) show the y_D^- distributions in water obtained with the simulated 3D Bridge SOI microdosimeter for incident 176.8 MeV proton beams. The y_D^- values were about 4 keV/µm at the plateau region and around 7 to 14 keV/µm at the BP region. In the tail region, y_D^- values were increasing from 5 keV/µm to 10 keV/µm at depths 224 mm to 250 mm.

Figure 4 (a) and (b) show the derived RBE_{10} values for mono-energetic 176.8 MeV proton beams. The simulated RBE_{10} values were 0.99 ± 0.02 in the plateau region (up to 150 mm depth). In the BP region, RBE_{10} values ranged from 1.05 ± 0.01 to 1.22 ± 0.07. In the tail region, RBE_{10} values also increased with increasing y_D^- values from 1.03 ± 0.12 to 1.12 ± 0.24 at depths 224 mm to 250 mm. This increasing RBE_{10} may affect healthy tissue or OAR, particularly those near the tumour.

Table 1 presents the y_F^-, y_D^-, and RBE_{10} of mono-energetic 176.8 MeV proton beams obtained by simulating the 3D Bridge Microdosimeter at different depths, ranging from 32 mm to 250 mm. The maximum RBE_{10} value is 1.22 occurred at a depth of 214 mm, which is 9 mm after the pinnacle of the BP. At the maximum physical dose at a depth of 205 mm, the RBE_{10} value is approximately 1.05 and y_D^- is 6.85 ± 0.14 keV/µm. The maximum y_D^- is 9.41 ± 0.63 keV/µm, and derived RBE_{10} is 1.22 ± 0.07 at a depth of 214 mm.

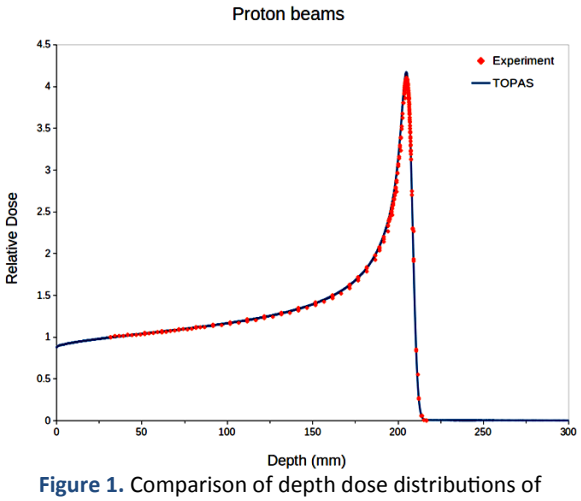

Figure 1. Comparison of depth dose distributions of mono-energetic 176.8 MeV proton beams obtained with TOPAS simulation and experimental data.

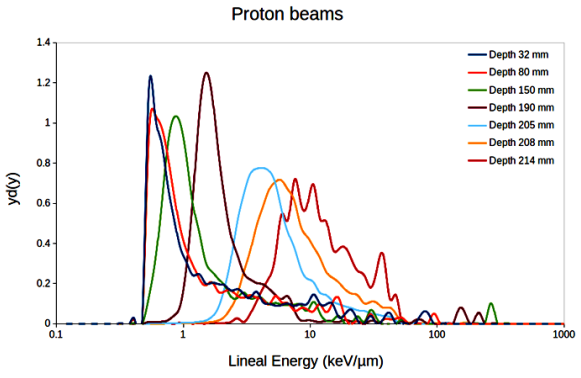

Figure 2. Microdosimetric spectra of lineal energy of mono-energetic 176.8 MeV proton beams at each depth in a water phantom.

[DOI: 10.61186/ijrr.22.3.703]

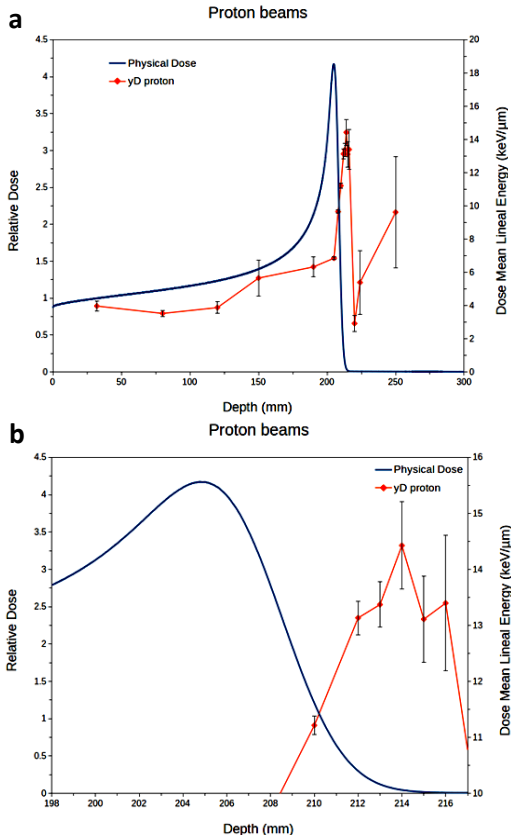

Figure 3. (a) Dose mean lineal energy y_D^- of mono-energetic 176.8 MeV proton beams derived from SOI Bridge microdosimeter as a function of depth in a water phantom **(b)** zoom view.

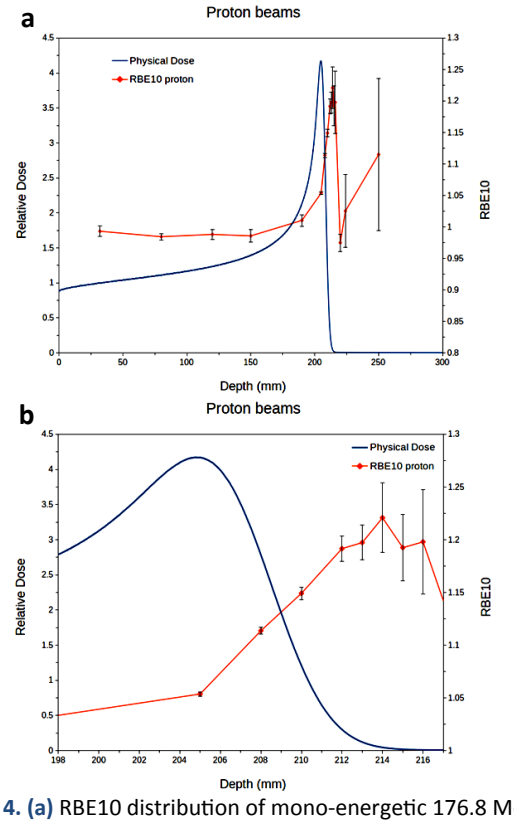

Figure 4. (a) RBE10 distribution of mono-energetic 176.8 MeV proton beams as a function of depth in a water phantom **(b)** zoomed view.

Table 1. Simulated microdosimetric quantities and RBE10 values of mono-energetic 176.8 MeV proton beams in water.

Depth (mm)	Frequency mean lineal energy y_F^- (keV/µm)	Dose mean lineal energy y_D^- (keV/µm)	Relative Biological Effectiveness at a 10% survival fraction (RBE_{10})
32	0.99 ± 0.03	3.97 ± 0.61	0.99 ± 0.02
80	0.97 ± 0.03	3.53 ± 0.37	0.98 ± 0.01
120	1.02 ± 0.02	3.88 ± 0.71	0.99 ± 0.02
150	1.14 ± 0.02	5.66 ± 2.15	0.99 ± 0.02
190	1.83 ± 0.03	6.33 ± 1.19	1.01 ± 0.02
205	4.37 ± 0.02	6.85 ± 0.14	1.05 ± 0.00
208	6.08 ± 0.05	9.65 ± 0.20	1.11 ± 0.01
210	7.27 ± 0.10	11.21 ± 0.32	1.15 ± 0.01
212	8.48 ± 0.23	13.13 ± 0.60	1.19 ± 0.02
213	8.80 ± 0.32	13.37 ± 0.81	1.20 ± 0.03
214	9.41 ± 0.63	14.43 ± 1.56	1.22 ± 0.07
215	9.28 ± 0.77	13.11 ± 1.54	1.19 ± 0.06
216	7.26 ± 0.99	13.40 ± 2.42	1.20 ± 0.10
220	1.95 ± 0.52	2.92 ± 0.99	0.97 ± 0.03
224	2.35 ± 1.16	5.39 ± 3.81	1.03 ± 0.12
250	3.81 ± 1.43	9.62 ± 6.73	1.12 ± 0.24

Mono-energetic 176.4 MeV/µm helium ion beams

Figure 5 presents Bragg curves of incident 176.4 MeV/µm helium ion beams. The position of the BP of helium ion simulation occurs at a depth of 206.90 mm, and NSRL experimental data appears at a depth of 206.65 mm. The difference between the simulation and experiment is 0.25 mm due to positioning uncertainty.

Figure 6 displays the microdosimetric spectra distributions of incident 176.4 MeV/µm helium ion beams. These distributions are represented in terms of lineal energy. The data presented in the figure was converted from silicon to water utilising the 3D Bridge microdosimeter. As depth increased, the peak of the spectra appeared to move towards higher lineal energies, indicating increased LET of incident ions and contribution from secondary particles in the water phantom.

Figure 7 (a) and (b) show simulated y_D^- distributions in water obtained with the 3D Bridge SOI microdosimeter for incident 176.4 MeV/µm helium ion beams. The y_D^- values were about 4 to 8 keV/µm at the plateau region and around 35 to 56 keV/µm at the BP region. In the tail region y_D^- values were increasing from 7 keV/µm to 14 keV/µm at depths 224 mm to 250 mm. The reason for this was that the proportion of secondary fragments became more significant as depth increases in the tail region.

Figure 8 (a) and (b) show the derived RBE_{10} for mono-energetic 176.4 MeV/u helium ion beams. The RBE_{10} value is 1.04 ± 0.01 in the plateau region at 32 mm depth. In the BP region, RBE_{10} values range from 1.64 ± 0.03 to a maximum of 2.04 ± 0.15 at a depth of 210 mm, approximately 3 mm after the maximum physical dose. A zoom view of the RBE_{10} values and the physical dose at the BP can be seen in figure 8 (b). After reaching the maximum RBE_{10} value at a depth of 210 mm, it can be observed that the RBE_{10} values decreased to 1.04 ± 0.02 at the distal part, at a depth of 214 mm. The decrease in RBE_{10} towards the distal

[DOI: 10.61186/ijrr.22.3.703]

part of the BP can be attributed to the overkilling effect of cells, which has been was considered in the MK model [7]. As the y_D^- values rose in the tail region, the RBE_{10} values also increased from 1.03 ± 0.02 to 1.07 ± 0.06 at depths ranging from 224 mm to 250 mm. This increasing RBE_{10} could affect healthy tissue or OAR.

Table 2 presents the y_F^-, y_D^- and RBE_{10} of mono-energetic 176.4 MeV/µm helium ion beams obtained by simulating the 3D Bridge SOI microdosimeter at different depths, ranging from 32 mm to 250 mm. It shows that the uncertainty of y_D^- for the helium ion is lower compared to that of the proton when considering the same number of histories and configurations. This result is in agreement with the findings of Parisi *et al.* [36]. The uncertainty of y_D^- decreases as the charged particle becomes heavier. This is because heavier ions possess greater stopping powers, which reduce the occurrence of nuclear reaction events. This is due to the fact that the energy deposited by primary particles and secondary fragments became more closely aligned.

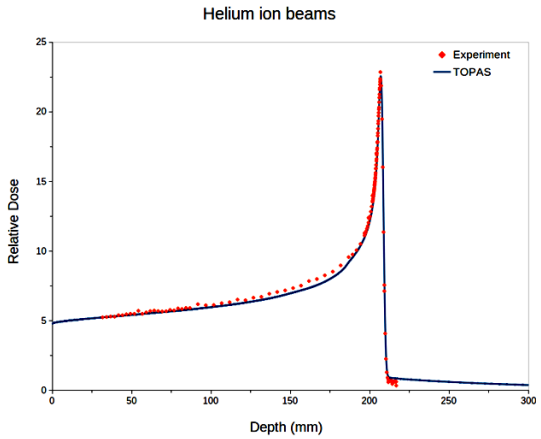

Figure 5. Comparison of depth dose distributions of mono-energetic 176.4 MeV/µm helium ion beams obtained with TOPAS simulation and experimental data.

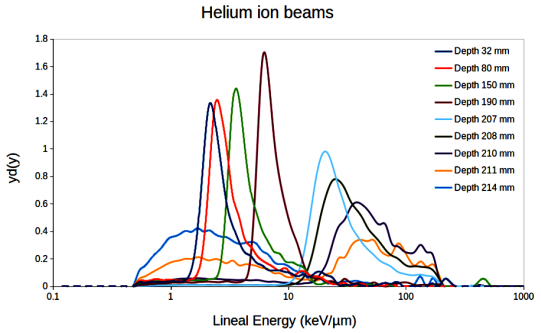

Figure 6. Microdosimetric spectra of lineal energy of mono-energetic 176.4 MeV/µm helium ion beams at each depth in a water phantom.

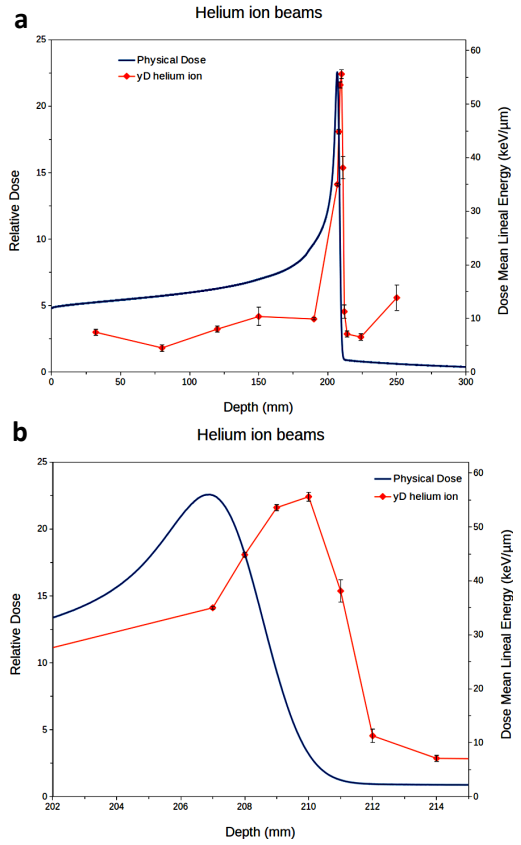

Figure 7. (a) Dose mean lineal energy of mono-energetic 176.4 MeV/µm helium ion beams deriving from SOI Bridge microdosimeter as a function of depth in a water phantom **(b)** zoom view.

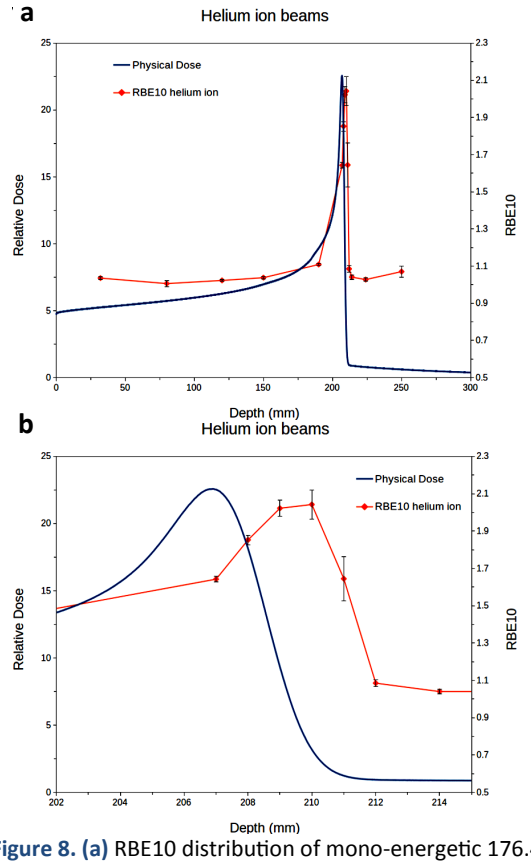

Figure 8. (a) RBE10 distribution of mono-energetic 176.4 MeV/µm helium ion beams as a function of depth in a water phantom **(b)** zoom view.

[DOI: 10.61186/ijrr.22.3.703]

Table 2. Simulated Microdosimetric quantities of mono-energetic 176.4 MeV/u helium ion beams in water.

Depth (mm)	Frequency mean lineal energy y_F^- (keV/µm)	Dose mean lineal energy y_D^- (keV/µm)	Relative Biological Effectiveness at a 10% survival fraction (RBE_{10})
32	2.62 ± 0.04	7.41 ± 1.08	1.04 ± 0.02
80	2.75 ± 0.06	4.50 ± 1.24	1.01 ± 0.03
120	3.13 ± 0.03	8.01 ± 1.19	1.02 ± 0.01
150	3.69 ± 0.05	10.36 ± 3.43	1.04 ± 0.01
190	6.01 ± 0.07	9.89 ± 0.42	1.11 ± 0.01
207	19.22 ± 0.13	35.01 ± 0.52	1.64 ± 0.03
208	22.04 ± 0.16	44.85 ± 0.77	1.85 ± 0.05
209	20.06 ± 0.22	53.58 ± 1.09	2.02 ± 0.09
210	10.69 ± 0.23	55.61 ± 1.66	2.04 ± 0.15
211	3.64 ± 0.15	38.12 ± 4.19	1.64 ± 0.24
212	1.99 ± 0.04	11.27 ± 2.43	1.09 ± 0.04
214	1.87 ± 0.04	7.09 ± 1.10	1.04 ± 0.02
224	1.82 ± 0.04	6.51 ± 1.20	1.03 ± 0.02
250	1.88 ± 0.06	13.86 ± 4.76	1.07 ± 0.06

DISCUSSION

The y_D^- value of mono-energetic 176.8 MeV proton beam at a depth of 32 mm (plateau region) in water was measured to be 3.97 ± 0.61 keV/µm. As the depth increased, the y_D^- value gradually rose, reaching its peak at 14.43 ± 1.56 keV/µm when the depth reached 214 mm (distal part of the BP). It is notable that the maximum y_D^- occurred about 9 mm after the maximum physical dose. In the tail region y_D^- values increased from 5 keV/µm to 10 keV/µm at depths 224 mm to 250 mm. It is due to the increasing contribution of secondary fragments at respective depths. The maximum y_D^- value occurred beyond the maximum physical dose, as determined with TOPAS-based simulations. This observation is consistent with the experimental work by Linh *et al.* [37]. Beyond the BP, incident protons have lost a significant portion of their energy, leading to a diminished ability to deposit energy. However, y_D^- may continue to increase due to nuclear interactions events occurring in a confined region. The increased in nuclear interaction events contributes to a higher y_D^- even as the total deposited energy decreases beyond the BP.

High uncertainty of y_D^- in the tail region of proton beam was due to rare nuclear interactions in the SV of the detector discovered to impair microdosimetric uncertainties unless very high statistics are gathered significantly. Parisi *et al.* [36] found that such occurrences had a growing effect on increasing beam energy and lighter ions. The RBE_{10} values of protons vary from 0.99 to 1.22, in contrast with the clinical TPS of proton therapy typically implements a constant RBE of 1.1.

The maximum RBE_{10} value for proton is 1.22 at depth 214 mm which is 9 mm after the maximum physical dose. In contrast, the maximum RBE_{10} value for helium ions is 2.04 at a depth of 210 mm, which is around 3 mm after the maximum physical dose. Overall, the RBE_{10} values for helium ions were higher than the case of proton at the entrance, BP region and in the distal part of the BP. The position of maximum RBE_{10} value for helium ions is also closer to the maximum physical dose compared to the case of protons, this should be taken into consideration because the damage to the tumours and organs depends on the RBE rather than the physical dose. With respect to protons, helium ions produce higher secondary fragmentations, and a high number of nuclear isotopes have a significant impact on the RBE, especially beyond the BP and in the out-of-field region, this could potentially harm the OAR. Therefore, the accuracy of fragmentation in the physical models used in simulation is of high importance. Further verification with experimental data of the physical models available in the TOPAS is required.

The utilisation of helium ions for treating cancerous tumours has garnered increasing global attention as an alternative to protons and carbon ions. More research studies specifically dedicated to helium ions are imperative [38]. These results further highlight the potential advantages of utilising helium ions in cancer treatment. Helium ions exhibit higher RBE_{10} values and are positioned closer to the maximum dose at the BP compared to protons. These findings of the study offer valuable insights for precise biological dose prediction, particularly when targeting the tumour in close proximity to OAR.

CONCLUSION

The RBE_{10} values for protons exhibit a range of 0.99 to 1.22, which differs from the standard practice of using a fixed RBE of 1.1 in the TPS for proton therapy. The simulation results in this study may be used as an outlook for radiobiological experiments in the NSRL. The study also presented a fast and reliable radiation field characterisation and RBE prediction tool for charged particle beams using TOPAS MC-based simulations toolkit. Future work will focus on investigating the microdosimetric spectra of the secondary fragments.

ACKNOWLEDGMENT

The authors are grateful to Dr. Michael Sivertz for providing Bragg curves experimental data of NASA Space Radiation Laboratory.

Ethical Considerations: Not applicable.

Funding: This work was supported by the Ministry of Higher Education Malaysia for Fundamental Research Grant Scheme (FRGS) with Project Code: FRGS / 1 / 2019/ STG02 / USM / 02 / 7. Malaysia International Scholarship (MIS) is acknowledged for the scholarship to the first author.

Conflicts of interests: The authors declare no conflict of interest.

Author contributions: The authors confirm contribution to the manuscript as follows:

[DOI: 10.61186/ijrr.22.3.703]

conceptualization: M.A.E., D.S., and Y.C.K.; methodology: M.A.E., D.S., and Y.C.K.; writing original draft preparation: M.A.E.; writing review and editing: D.S., and Y.C.K. supervision: D.S., and Y.C.K. All authors have read and agreed to the manuscript.

REFERENCES

1. Ekinci F, Bostanci E, Güzel MS, Dagli O (2023) Simulation based analysis of 4He, 7Li, 8Be and 10B ions for heavy ion therapy. *International Journal of Radiation Research*, ***21(1):*** *131-137.*
2. Mohan R (2022) A review of proton therapy – Current status and future directions. *Precision Radiation Oncology,* ***6(2):*** *164-176.*
3. Ebner DK, Frank SJ, Inaniwa T, Yamada S & Shirai T (2021) The Emerging Potential of Multi-Ion Radiotherapy. *Frontiers in Oncology*, ***11****.*
4. La Tessa C, Sivertz M, Chiang IH, Lowenstein D & Rusek A (2016) Overview of the NASA space radiation laboratory. *Life Sciences in Space Research*, ***11*****:** *18-23.*
5. Held KD, Blakely EA, Story MD & Lowenstein DI (2016) Use of the NASA Space Radiation Laboratory at Brookhaven National Laboratory to Conduct Charged Particle Radiobiology Studies Relevant to Ion Therapy. *Radiation Research*, ***185(6):*** *563-567.*
6. Burigo L, Gehrke T, J kel O, Sivertz M, Olsen T, Rusek A, Obcemea C & Greilich S (2020) Beam characterization at NSRL for radiobiological experiments. *Phase 1. Journal of Instrumentation*, ***15(10):*** *T10004.*
7. Kase Y, Kanai T, Matsumoto Y, Furusawa Y, Okamoto H, Asaba T, Sakama M & Shinoda H (2006) Microdosimetric measurements and estimation of human cell survival for heavy-ion beams. *Radiation Research*, ***166(4):*** *629-638.*
8. Newhauser W (2009) International Commission on Radiation Units and Measurements Report 78: Prescribing, Recording and Reporting Proton-beam Therapy. *Radiation Protection Dosimetry*, ***133(1):*** *60-62.*
9. Mohan R, Peeler CR, Guan F, Bronk L, Cao W & Grosshans DR (2017) Radiobiological issues in proton therapy. *Acta Oncologica,* ***56(11):*** *1367-1373*
10. Zaider M (1991) Elements of microdosimetry. *Medical Physics*, ***18 (6):*** *1085-1092.*
11. De Nardo L, Cesari V, Donà G, Magrin G, Colautti P, Conte V & Tornielli G (2004) Mini-TEPCs for radiation therapy. *Radiation Protection Dosimetry*, ***108(4):*** *345-352.*
12. Verona C, Magrin G, Solevi P, Bandorf M, Marinelli M, Stock M & Verona Rinati G (2018) Toward the use of single crystal diamond based detector for ion-beam therapy microdosimetry. *Radiation Measurements*, ***110:*** *25-31.*
13. Agosteo S, Fallica PG, Fazzi A, Pola A, Valvo G & Zotto P (2005) A feasibility study of a solid-state microdosimeter. *Applied Radiation and Isotopes*, ***63(5-6 SPEC. ISS.):*** *529-535.*
14. Galer S, Hao L, Gallop J, Palmans H, Kirkby K & Nisbet A (2011) Design concept for a novel SQUID-based microdosemeter. *Radiation Protection Dosimetry*, ***143(2-4):*** *427-431.*
15. Bradley PD, Rosenfeld AB, Allen B, Coderre J & Capala J (1999) Performance of silicon microdosimetry detectors in boron neutron capture therapy. *Radiation Research*, ***151(3):*** *235-243.*
16. Nikjoo H (2003). Radiation track and DNA damage. *International Journal of Radiation Research*, ***1(1):*** *14-17.*
17. Fassó A, Ferrari A, Sala PR & Ranft J (2001) FLUKA: Status and prospects for hadronic applications. *Advanced Monte Carlo for Radiation Physics, Particle Transport Simulation and Applications (pp. 955-960), Springer.*
18. Agostinelli S, Allison J, Amako K, Apostolakis J, Araujo H, Arce P, *et al.* (2003) GEANT4 - A simulation toolkit. *Nuclear Instruments and Methods in Physics Research, Section A: Accelerators, Spectrometers, Detectors and Associated Equipment*, ***506(3):*** *250-303.*
19. Allison J, Amako K, Apostolakis J, Araujo H, Dubois PA, Asai M, *et al.* (2006) Geant4 developments and applications. *IEEE Transactions on Nuclear Science*, ***53(1):*** *270-278.*
20. Allison J, Amako K, Apostolakis J, Arce P, Asai M, Aso T, *et al.* (2016) Recent developments in GEANT4. *Nuclear Instruments and Methods in Physics Research, Section A: Accelerators, Spectrometers, Detectors and Associated Equipment*, ***835:*** *186-225.*
21. Ganjeh AZ, Eslami-Kalantari M, Ebrahimi Loushab M, Mowlavi AA (2020) Investigation of the direct DNA damages irradiated by protons of different energies using geant4-DNA toolkit. *International Journal of Radiation Research*, ***18(4):*** *809-815.*
22. Goorley T, James M, Booth T, Brown F, Bull J, Cox LJ, *et al.* (2012) Initial MCNP6 release overview. *Nuclear Technology,* ***180(3):*** *298-315.*
23. Pshenichnov, I, Mishustin, I, & Greiner, W (2007) MCHIT - Monte Carlo model for proton and Heavy-Ion Therapy. *International Conference on Nuclear Data for Science and Technology, 1343–1346.*
24. Burigo L, Pshenichnov I, Mishustin I & Bleicher M (2013) Microdosimetry of radiation field from a therapeutic 12C beam in water: A study with Geant4 toolkit. *Nuclear Instruments and Methods in Physics Research, Section B: Beam Interactions with Materials and Atoms*, ***310:*** *37-53.*
25. Zhu H, Chen Y, Sung W, McNamara AL, Tran LT, Burigo LN, *et al*. (2019) The microdosimetric extension in TOPAS: Development and comparison with published data. *Physics in Medicine and Biology*, ***64(14):*** *15.*
26. Bolst D, Guatelli S, Tran LT, Chartier L, Davis J, Biasi G, *et al*. (2020) Validation of Geant4 for silicon microdosimetry in heavy ion therapy. *Physics in Medicine and Biology*, ***65(4):*** *045014.*
27. Taddei PJ, Zhao Z & Borak TB (2008) A comparison of the measured responses of a tissue-equivalent proportional counter to high energy heavy (HZE) particles and those simulated using the Geant4 Monte Carlo code. *Radiation Measurements*, ***43(9-10):*** *1498-1505.*
28. Eulitz J, Lutz B, Wohlfahrt P, Dutz A, Enghardt W, Karpowitz C, *et al.* (2019) A Monte Carlo based radiation response modelling framework to assess variability of clinical RBE in proton therapy. *Physics in Medicine and Biology*, ***64(22):*** *225020.*
29. Bronk L, Guan F, Patel D, Ma D, Kroger B, Wang X, *et al*. (2020) Mapping the relative biological effectiveness of proton, helium and carbon ions with high-throughput techniques. *Cancers*, ***12(12):*** *1-15.*
30. Mein S, Dokic I, Klein C, Tessonnier T, Böhlen TT, Magro G, *et al*. (2019) Biophysical modeling and experimental validation of relative biological effectiveness (RBE) for 4He ion beam therapy. *Radiation Oncology*, ***14(1):*** *1-16.*
31. Debrot E, Tra, L, Chartier L, Bolst D, Guatelli S, Vandevoorde C, *et al*. (2018) SOI microdosimetry and modified MKM for evaluation of relative biological effectiveness for a passive proton therapy radiation field. *Physics in Medicine and Biology*, ***63(23):*** *235007.*
32. Lee SH, Mizushima K, Yonai S, Matsumoto S, Mizuno H, Nakaji T, *et al.* (2022) Predicting the Biological Effects of Human Salivary Gland Tumour Cells for Scanned 4He-, 12C-, 16O- and 20Ne-Ion Beams Using an SOI Microdosimeter. *Applied Sciences*, ***12(12):*** *6148.*
33. Perl J, Shin J, Schümann J, Faddegon B & Paganetti H (2012) TOPAS: An innovative proton Monte Carlo platform for research and clinical applications. *Medical Physics*, ***39(11):*** *6818-6837.*
34. Faddegon B, Ramos-Méndez J, Schuemann J, McNamara A, Shin J, Perl J & Paganetti H (2020) The TOPAS tool for particle simulation, a Monte Carlo simulation tool for physics, biology and clinical research. *Physica Medica*, ***72(November 2019):*** *114-121.*
35. Bolst D, Guatelli S, Tran LT, Chartier L, Lerch MLF, Matsufuji N, Rosenfeld AB (2017) Correction factors to convert microdosimetry measurements in silicon to tissue in 12C ion therapy. *Physics in Medicine and Biology*, ***62(6):*** *2055-2069.*
36. Parisi G, Schettino G & Romano F (2022) A systematic study of the contribution of counting statistics to the final lineal energy uncertainty in microdosimetry. *Physics in Medicine and Biology*, ***67(15):*** *155002.*
37. Tran LT, Chartier L, Bolst D, Pogossov A, Guatelli S, Petasecca M, *et al*. (2017) Characterization of proton pencil beam scanning and passive beam using a high spatial resolution solid-state microdosimeter. *Medical Physics*, ***44(11):*** *6085-6095. https://doi.org/10.1002/mp.12563*
38. Horst F, Schardt D, Iwase H, Schuy C, Durante M, Weber U (2021) Physical characterization of 3He ion beams for radiotherapy and comparison with 4He. *Physics in Medicine and Biology*, ***66(9)****.*

[DOI: 10.61186/ijrr.22.3.703]